



Figures and figure supplements

Autophagy functions as an antiviral mechanism against geminiviruses in plants

Yakupjan Haxim et al

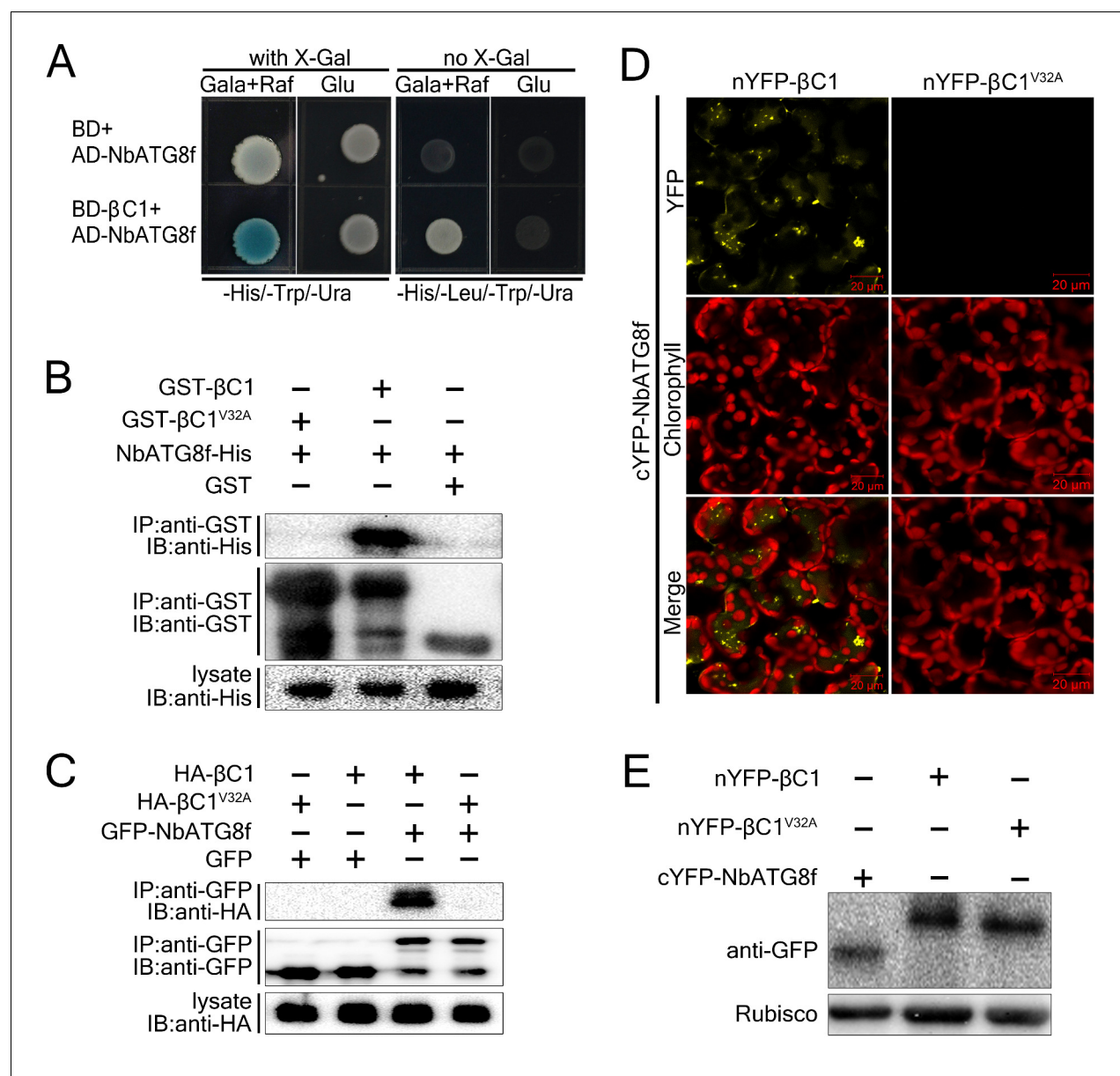


Figure 1. CLCuMuB β C1 interacts with NbATG8f in vivo and in vitro. (A) β C1 interacts with NbATG8f in yeast. SKY48 yeast strains containing AD-NbATG8f transformed with BD- β C1 or BD (control) were grown on Leu- selection plates at 28°C for 4 d. The positive interaction was indicated by the blue colony formation on X-gal-containing galactose (Gala) and raffinose (Raf) but not on plates containing glucose (Glu). (B) GST pull-down assay to show the in vitro interaction of NbATG8f with β C1, but not β C1^{V32A}. The total soluble proteins of *E. coli* expressing NbATG8f-6×His were incubated with GST- β C1 or GST- β C1^{V32A} immobilized on glutathione-sepharose beads and monitored by anti-His antibody. (C) β C1 was co-immunoprecipitated with NbATG8f. GFP-NbATG8f was transiently co-expressed with and HA- β C1 or its mutant HA- β C1^{V32A} in *N. benthamiana* leaves. At 60 hr post agroinfiltration (hpi), leaf lysates were immunoprecipitated with anti-GFP beads and then the precipitants were assessed by immunoblotting (IB) using anti-HA (upper panel) or anti-GFP antibodies (middle panel). (D) BiFC analyses in *N. benthamiana*. Representative images of nYFP- β C1 or nYFP- β C1^{V32A} BiFC co-expressed with cYFP-NbATG8f. (E) Western blot analyses of BiFC construct combinations from the same experiments as in (D). All combinations were detected with anti-GFP polyclonal antibody.

DOI: 10.7554/eLife.23897.003

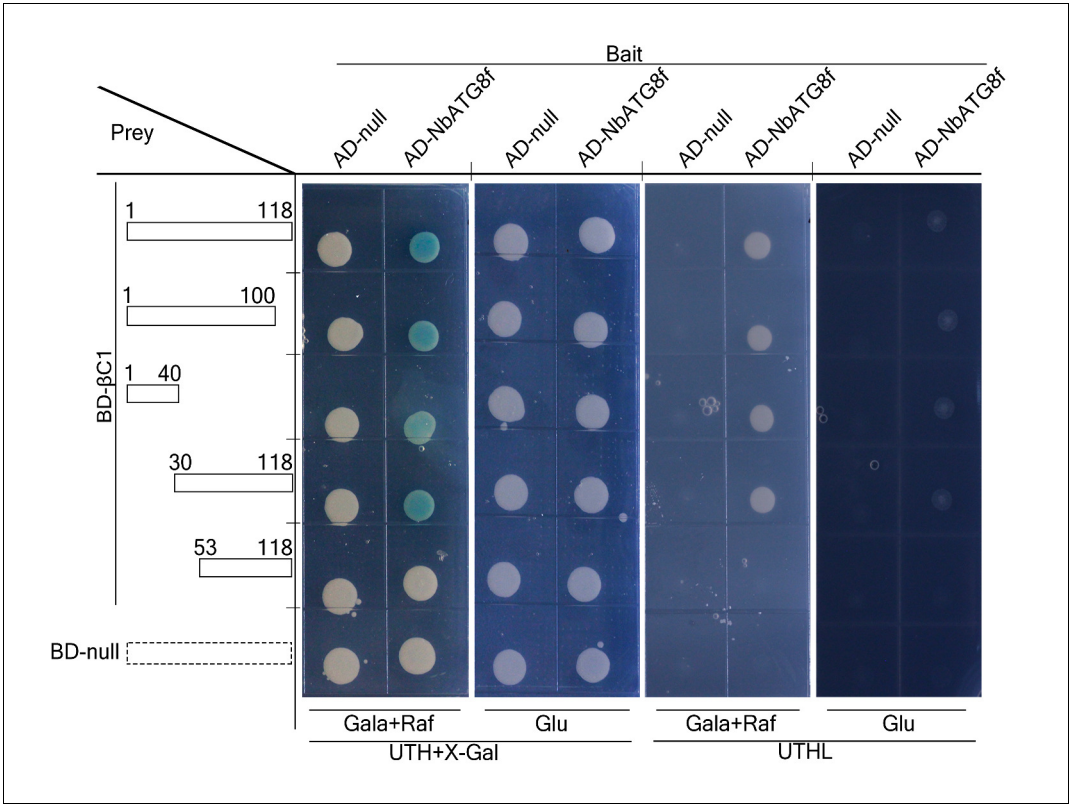
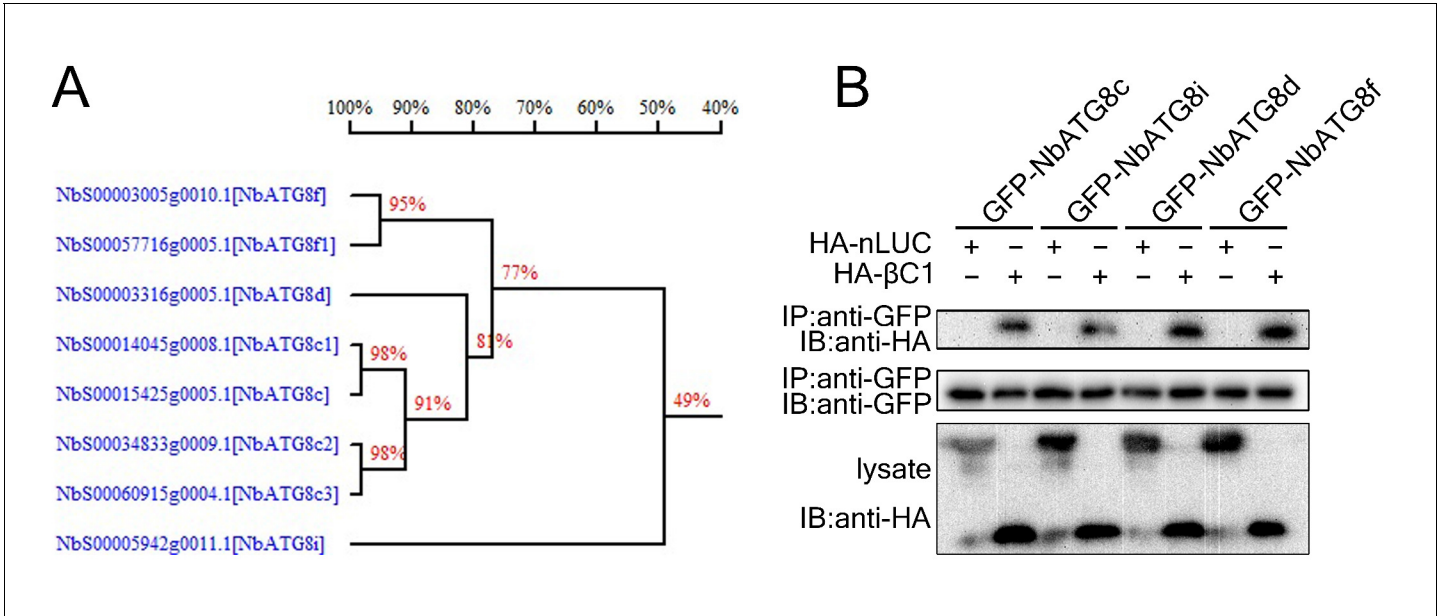


Figure 1—figure supplement 1. N terminus of β C1 is responsible for binding to NbATG8f. Schematic representation of the truncated mutants of β C1, their interactions with NbATG8f in yeast. Yeast cells transformed with four truncated mutants of β C1 and NbATG8f were selected on X-Gal-containing medium.
[DOI: 10.7554/eLife.23897.004](https://doi.org/10.7554/eLife.23897.004)



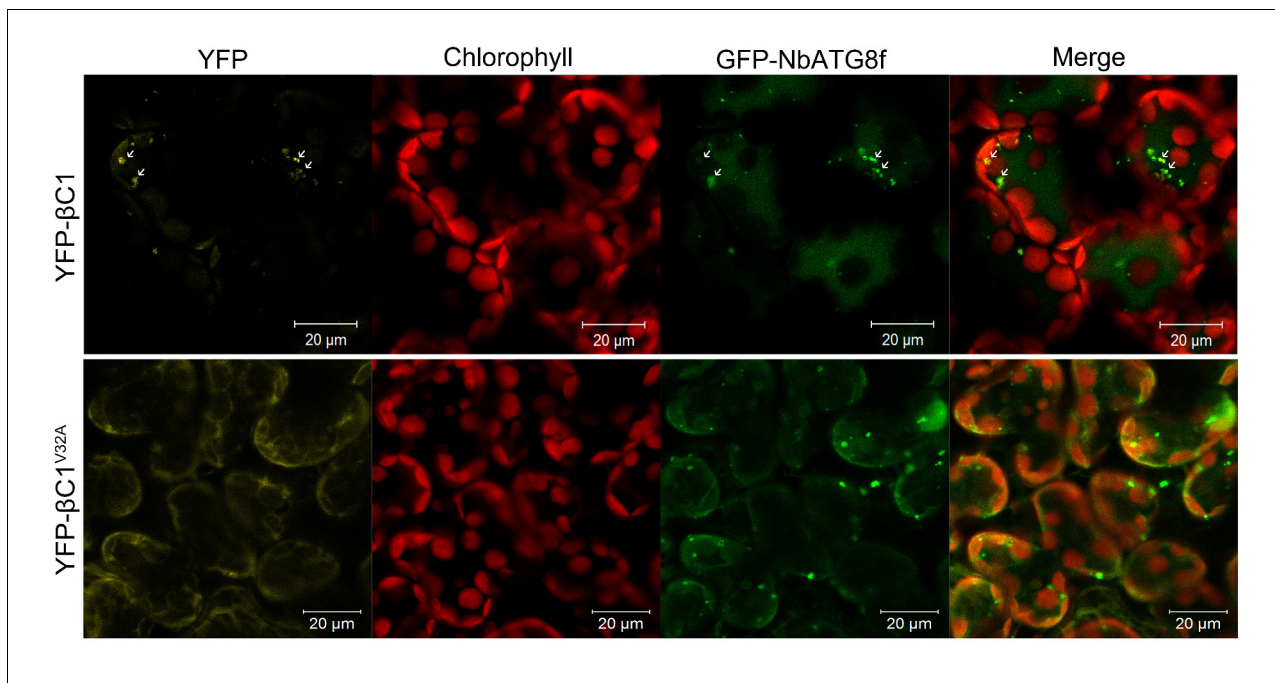


Figure 1—figure supplement 3. β C1 is co-localized with NbATG8f. CFP-NbATG8f was transiently co-expressed with YFP- β C1 or YFP- β C1^{V32A} in *N. benthamiana* leaves via agroinfiltration. The confocal microscope images of mesophyll cells were taken at 60 hpi.

DOI: [10.7554/eLife.23897.006](https://doi.org/10.7554/eLife.23897.006)

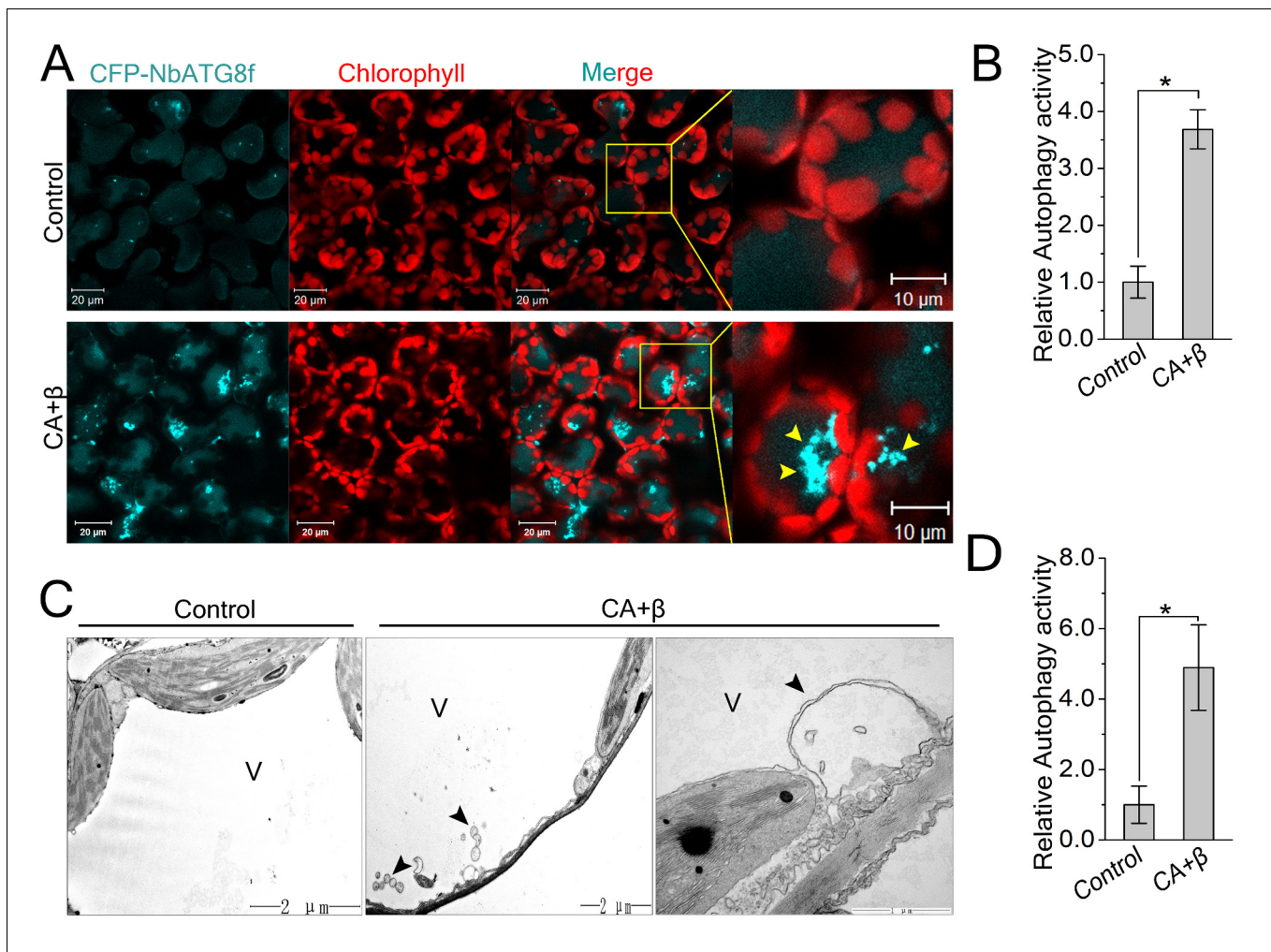


Figure 2. CLCuMuV infection activates autophagy. (A) Representative confocal microscopy images of dynamic autophagic activity revealed by specific autophagy marker CFP-NbATG8f in plants infected with CLCuMuV plus CLCuMuB (CA+β). (B) Quantification of the CFP-NbATG8f-labeled autophagic puncta per cell from (A). More than 500 mesophyll cells for each treatment were used for the quantification. Relative autophagic activity in virus infected plants was normalized to that of control plants, which was set to 1.0. Values represent means \pm SE from three independent experiments. (*) $p < 0.05$. (C) Representative TEM images of autophagic structures. Ultrastructure of autophagic bodies (arrows) was observed in the vacuoles of mesophyll cells of uninfected control and plants infected with CA+β. V for vacuole. (D) Autophagosome-like structures from (C) were quantified. At least 30 cells for each treatment were used for the quantification. Relative autophagic activity in virus infected plants was normalized to that of control plants, which was set to 1.0. Values represent means \pm SE from three independent experiments. (*) $p < 0.05$.

DOI: 10.7554/eLife.23897.009

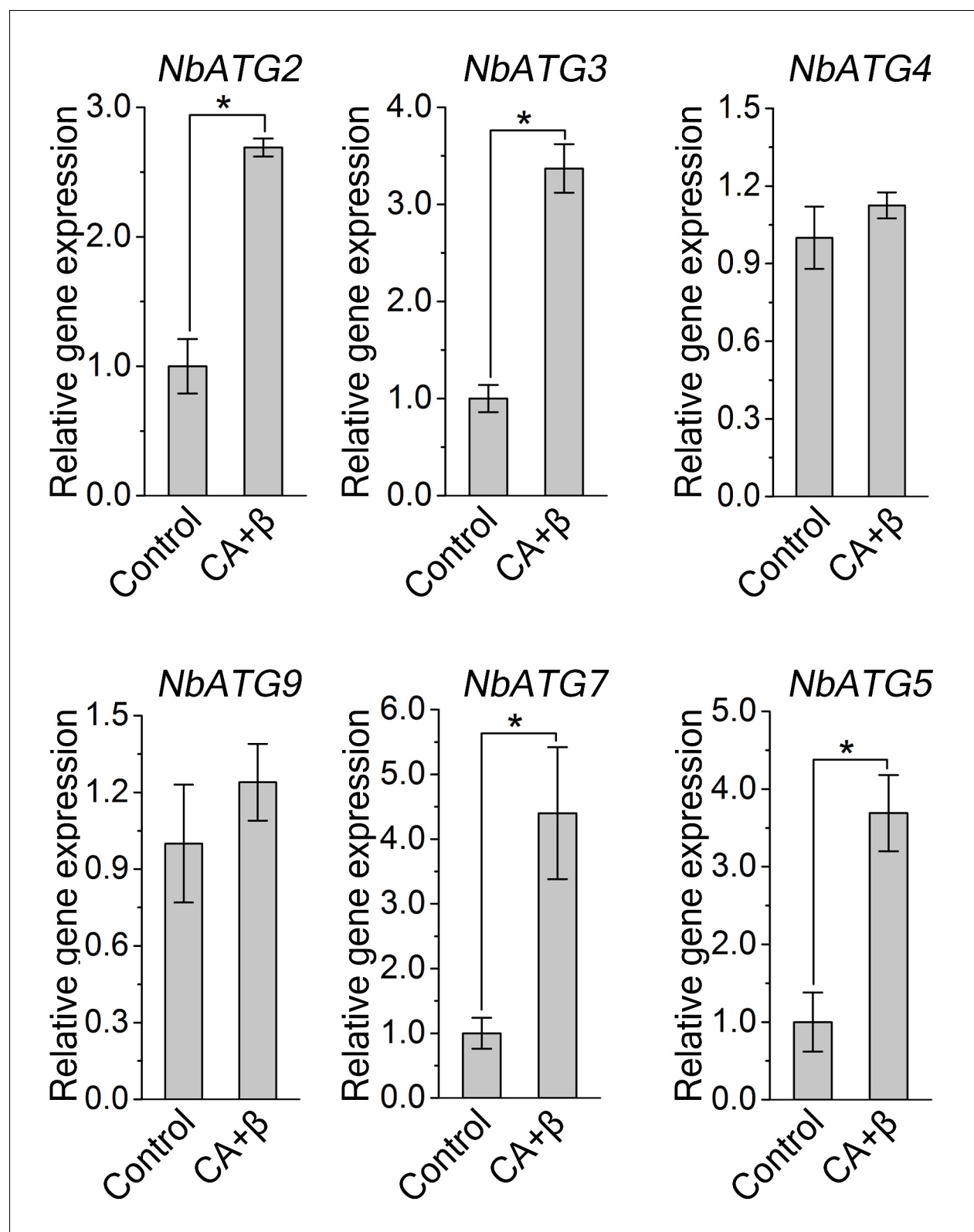


Figure 2—figure supplement 1. Transcription pattern of autophagy-related genes were altered during CLCuMuV infection. Quantitative RT-PCR was performed using total RNA isolated from the leaves of virus infected plants and non-infected plants. Expression data relative to non-infected plants are normalized to that of *Nbelf4α*. Values are means \pm SE from three independent experiments. (*) $p < 0.05$.

DOI: [10.7554/eLife.23897.010](https://doi.org/10.7554/eLife.23897.010)

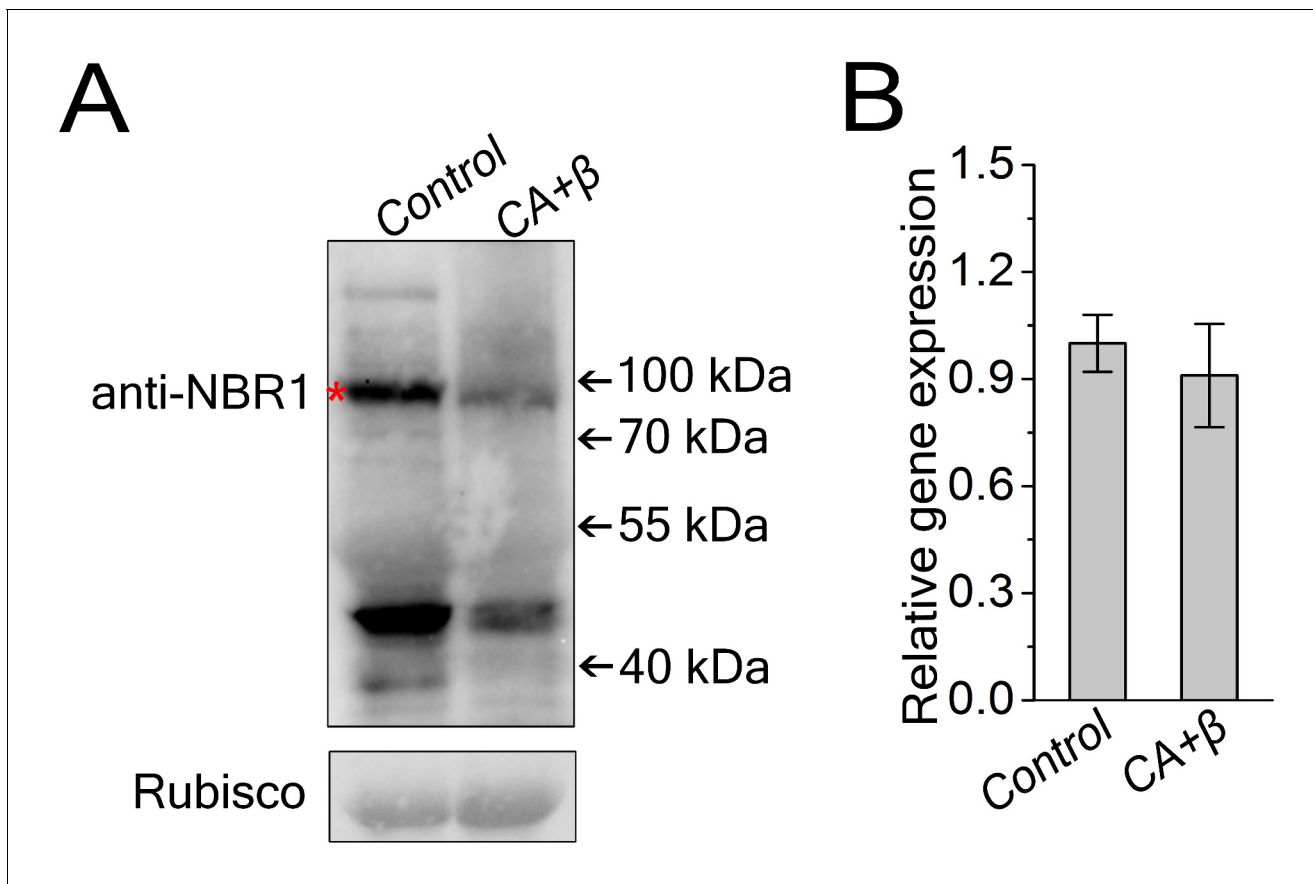


Figure 2—figure supplement 2. Viral infection decreased NbJoka2/NBR1 protein level. (A) Western blot assays showed that NbJoka2 protein level was reduced due to the increased autophagy flux in CLCuMuV-infected plants. NbJoka2 was detected with anti-NBR1 polyclonal antibody. Stars indicate expected band size. (B) mRNA level of *NbJoka2* was unchanged in CLCuMuV-infected plants. Real-time RT-PCR of *NbJoka2* was used to determine mRNA level. Values represent means \pm SE from three independent experiments. (*) $p < 0.05$.

DOI: [10.7554/eLife.23897.011](https://doi.org/10.7554/eLife.23897.011)

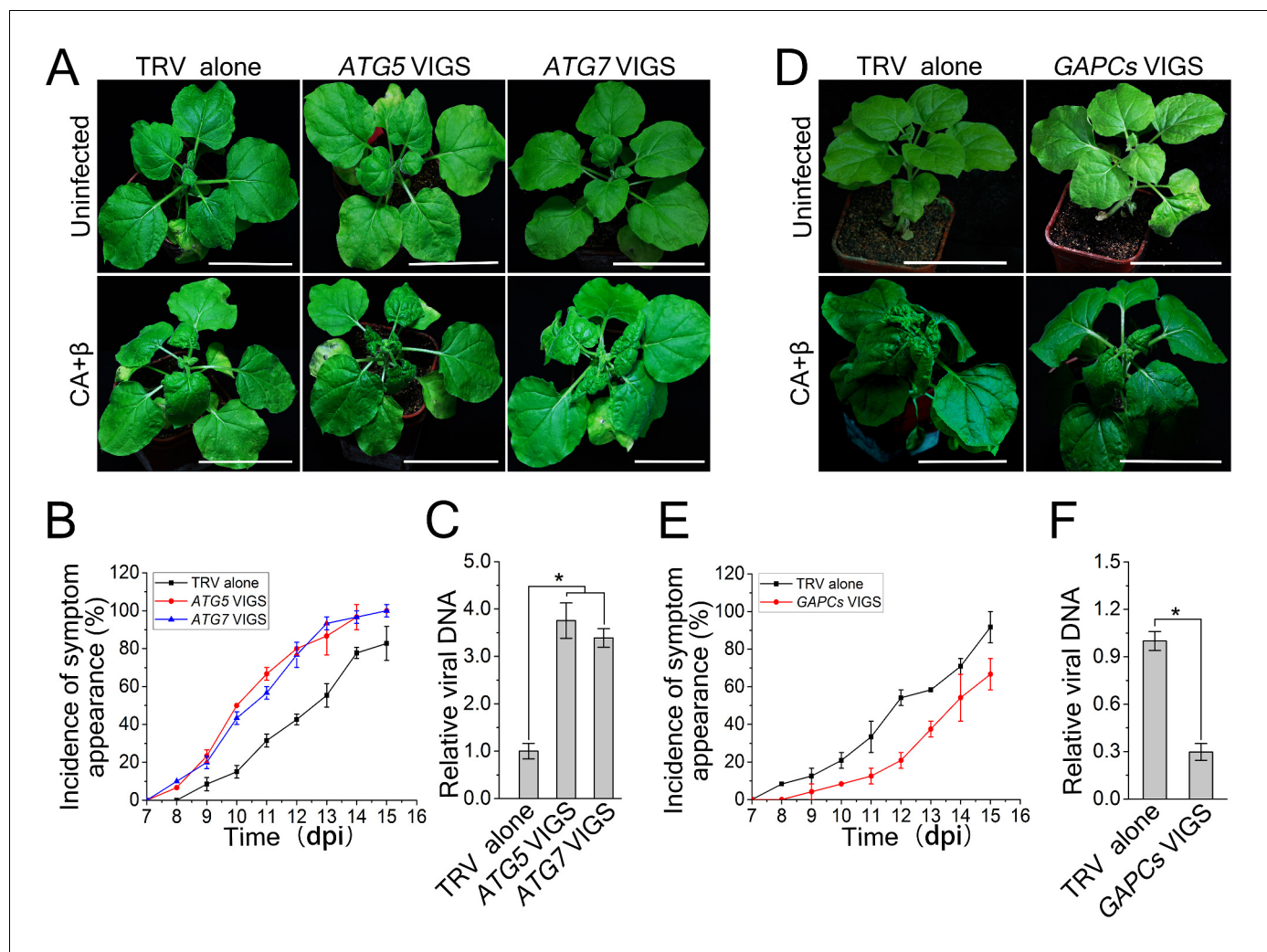


Figure 3. CLCuMuV DNA accumulation is affected by host cell autophagy. (A) Viral symptoms in ATG5- and ATG7-silenced plants infected with CLCuMuV plus CLCuMuB (CA+ β) at 12 dpi. Bar represents 7 cm. (B) The incidence of viral symptom appearance at different time points of post infection in ATG5- and ATG7-silenced plants. Symptom was indicated as the appearance of curled leaf caused by CA+ β . Values represent means \pm SE from three independent experiments. (C) Relative viral DNA accumulation in ATG5- and ATG7-silenced plants infected with CA+ β . Real-time PCR analysis of V1 gene from CLCuMuV was used to determine viral DNA level. Values represent means \pm SE from three independent experiments. (*) $p < 0.05$. (D) Viral symptoms in GAPCs-silenced plants infected with CA+ β at 15 dpi. Bar represents 7 cm. (E) The incidence of symptom appearance at different time points of post infection in GAPCs-silenced plants. Symptom was indicated as the appearance of curled leaf caused by CLCuMuV infection. Values represent means \pm SE from three independent experiments. (F) Relative viral DNA accumulation in GAPCs-silenced plants. Real-time PCR analysis of V1 gene from CLCuMuV was used to determine viral DNA level. Values represent means \pm SE from three independent experiments. (*) $p < 0.05$.

DOI: [10.7554/eLife.23897.012](https://doi.org/10.7554/eLife.23897.012)

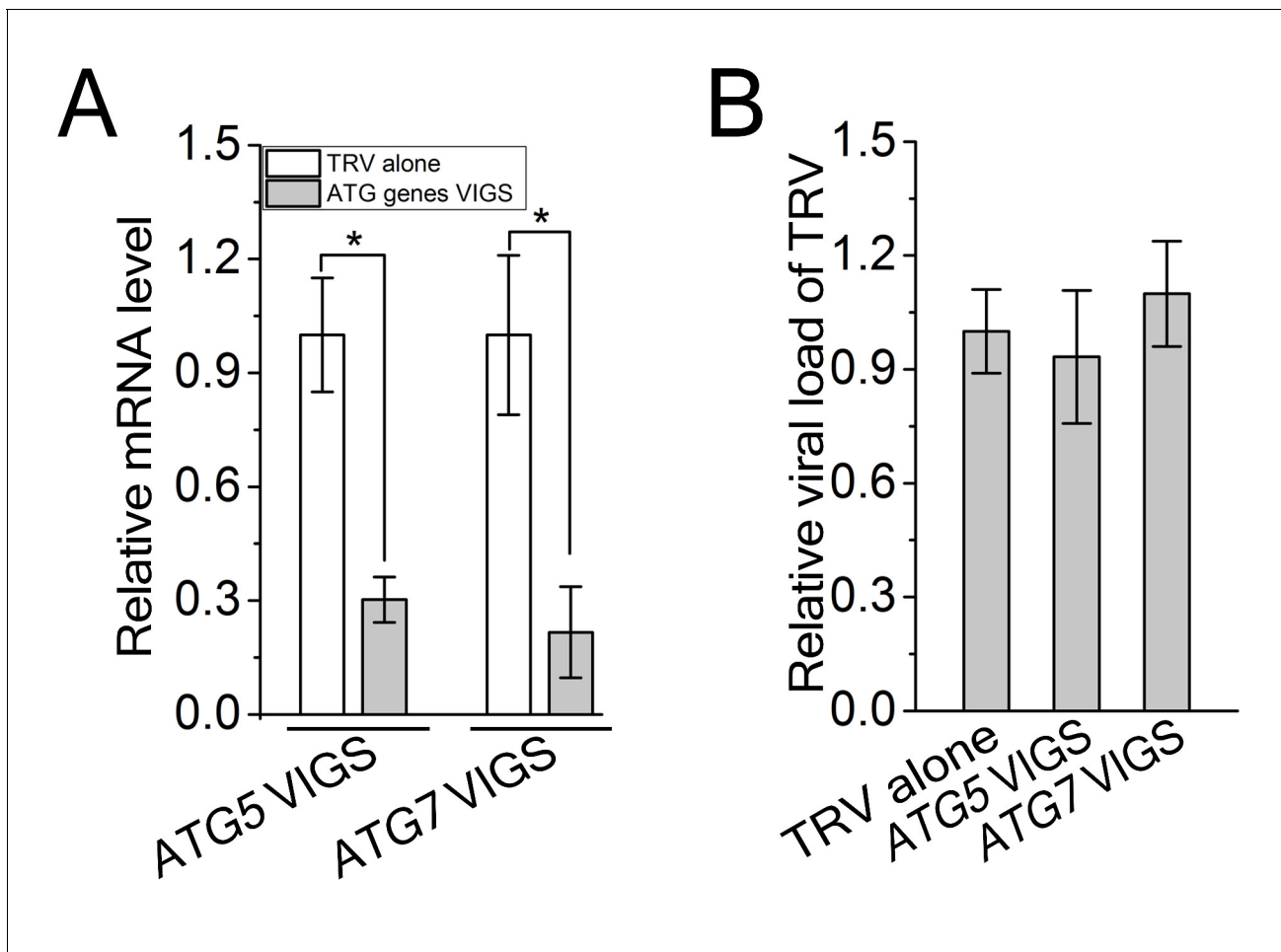


Figure 3—figure supplement 1. TRV viral titers were not changed during VIGS. (A) Reduced mRNA levels of ATG5 and ATG7 in the silenced plants. Real-time RT-PCR was performed using gene-specific primers. *Nbelf4α* was used as an internal control. Values are means \pm SE from three independent experiments. (B) Relative viral load of TRV in ATG5- and ATG7-silenced plants. Real-time PCR analysis of *CP* gene from TRV was used to determine viral load. Values represent means \pm SE from three independent experiments. (*) $p < 0.05$.

DOI: [10.7554/eLife.23897.013](https://doi.org/10.7554/eLife.23897.013)

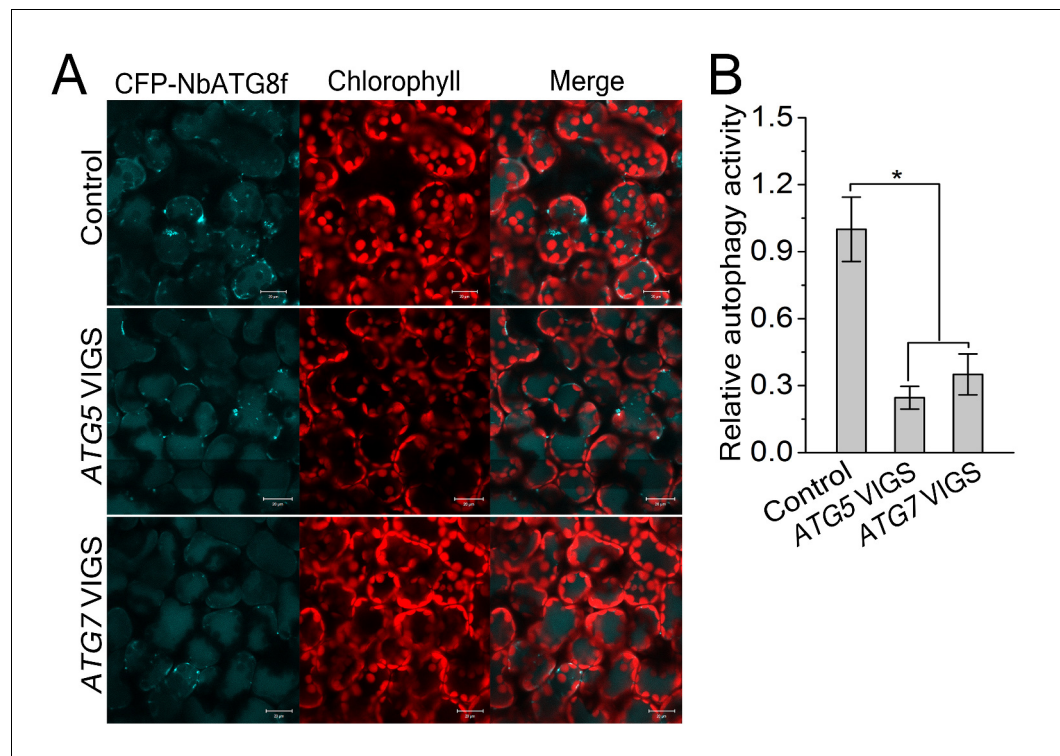


Figure 3—figure supplement 2. Involvement of *ATG5* and *ATG7* in autophagy is confirmed by VIGS. (A) Representative confocal images of dynamic autophagic activity revealed by specific autophagy marker CFP-NbATG8f in *ATG5*- and *ATG7*-silenced plants and control plants. (B) Reduced autophagic activity in *ATG5*- and *ATG7*-silenced plants. Quantification of the CFP-NbATG8f-labeled autophagic puncta per cell was performed. More than 500 mesophyll cells for each treatment were used for the quantification. Relative autophagic activity was normalized to that in TRV control plants, which was set to 1.0. Values represent means \pm SE from three independent experiments. (*) $p < 0.05$ compared with control.

DOI: [10.7554/eLife.23897.014](https://doi.org/10.7554/eLife.23897.014)

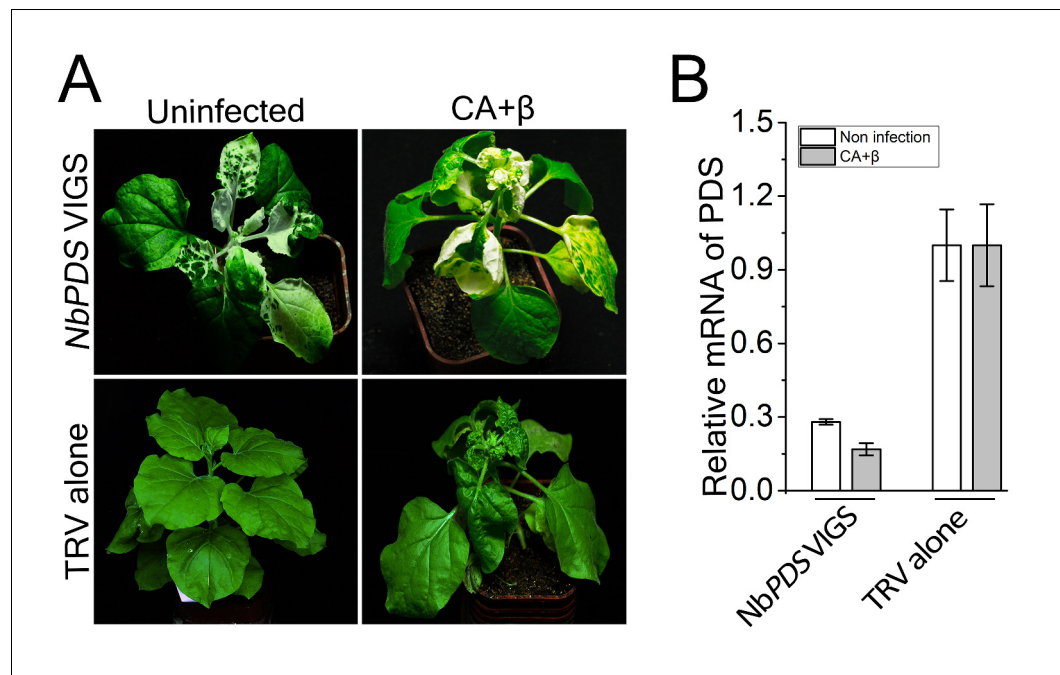


Figure 3—figure supplement 3. CLCuMuV infection has no effect on TRV-based VIGS of *NbPDS*. (A) TRV-based VIGS of *PDS* still caused a bleached phenotype in plants infected with CLCuMuV (CA) plus CLCuMuB (β) at 15 dpi. (B) Relative mRNA level of *NbPDS* in plants infected with CA+ β and non-infection. Leaf tissue was taken from *NbPDS*-silenced plants or control (TRV alone) at 15 dpi and total RNA was isolated. Real-time RT-PCR of *NbPDS* was used to determine mRNA level in virus infected or control plants. Values represent means \pm SE from three independent experiments.

DOI: [10.7554/eLife.23897.015](https://doi.org/10.7554/eLife.23897.015)

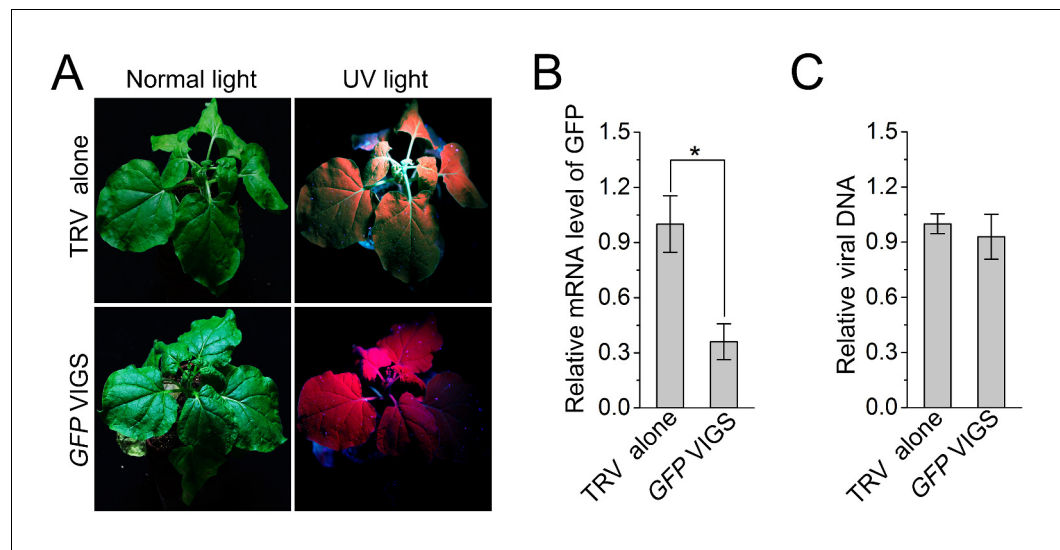


Figure 3—figure supplement 4. Silencing of a non-autophagy related gene *GFP* has no effect on CLCuMuV infection. **(A)** Viral symptom in *GFP*-silenced *N. benthamiana* *GFP*-transgenic16c line. The pictures were taken at 12 dpi. **(B)** mRNA level of *GFP* in *GFP*-silenced *N. benthamiana* *GFP*-transgenic16c line. Real-time RT-PCR was performed using *GFP*-specific primers. *eIF4α* was used as an internal control. Values are means \pm SE from three independent experiments. (*) $p < 0.05$. **(C)** Relative CLCuMuV DNA accumulation in *GFP*-silenced *N. benthamiana* *GFP*-transgenic16c line. Real-time PCR analysis of CLCuMuV *V1* gene was used to determine viral DNA level. Values represent means \pm SE from three independent experiments.

DOI: [10.7554/eLife.23897.016](https://doi.org/10.7554/eLife.23897.016)

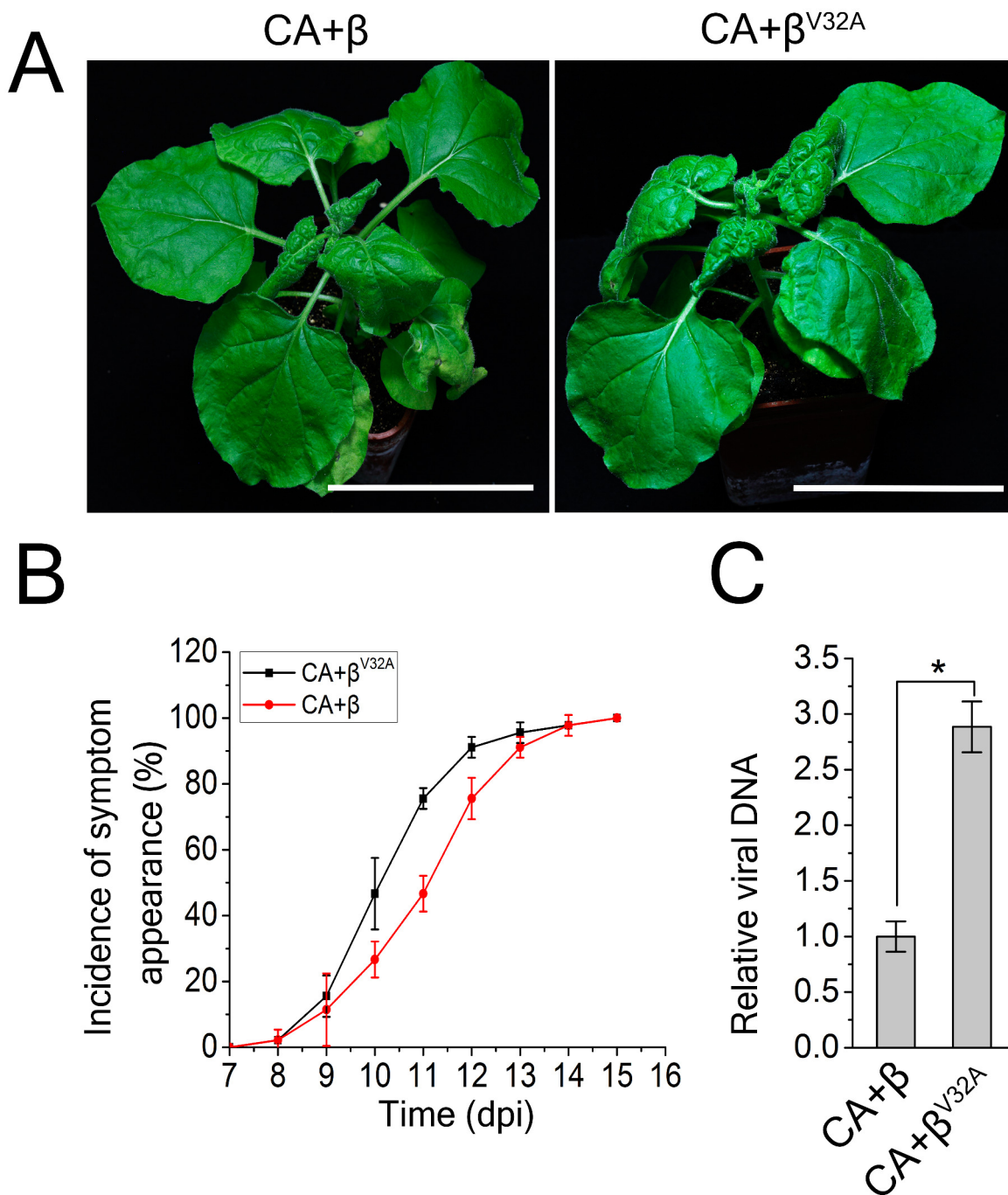


Figure 4. A V32A point mutation in β C1 enhanced CLCuMuV infection. (A) CLCuMuB mutant (β^{V32A}), which encodes a mutant β C1 V32A , caused the enhanced viral symptom compared to wild type CLCuMuB (β) when co-infected with CLCuMuV (CA). The pictures were taken at 12 dpi. A V32A point mutation in β C1 (β C1 V32A) eliminates its interaction with NbATG8f. (B) The incidence of symptom appearance at different time points of post infection. Symptom was indicated as the appearance of curled leaf caused by the infection with CA+ β or CA+ β^{V32A} . (C) Relative viral accumulation of CLCuMuV DNA. Real-time PCR analysis of V1 gene from CLCuMuV was used to determine viral DNA level. Values represent means \pm SE from three independent experiments. (*) $p < 0.05$.

DOI: 10.7554/eLife.23897.017

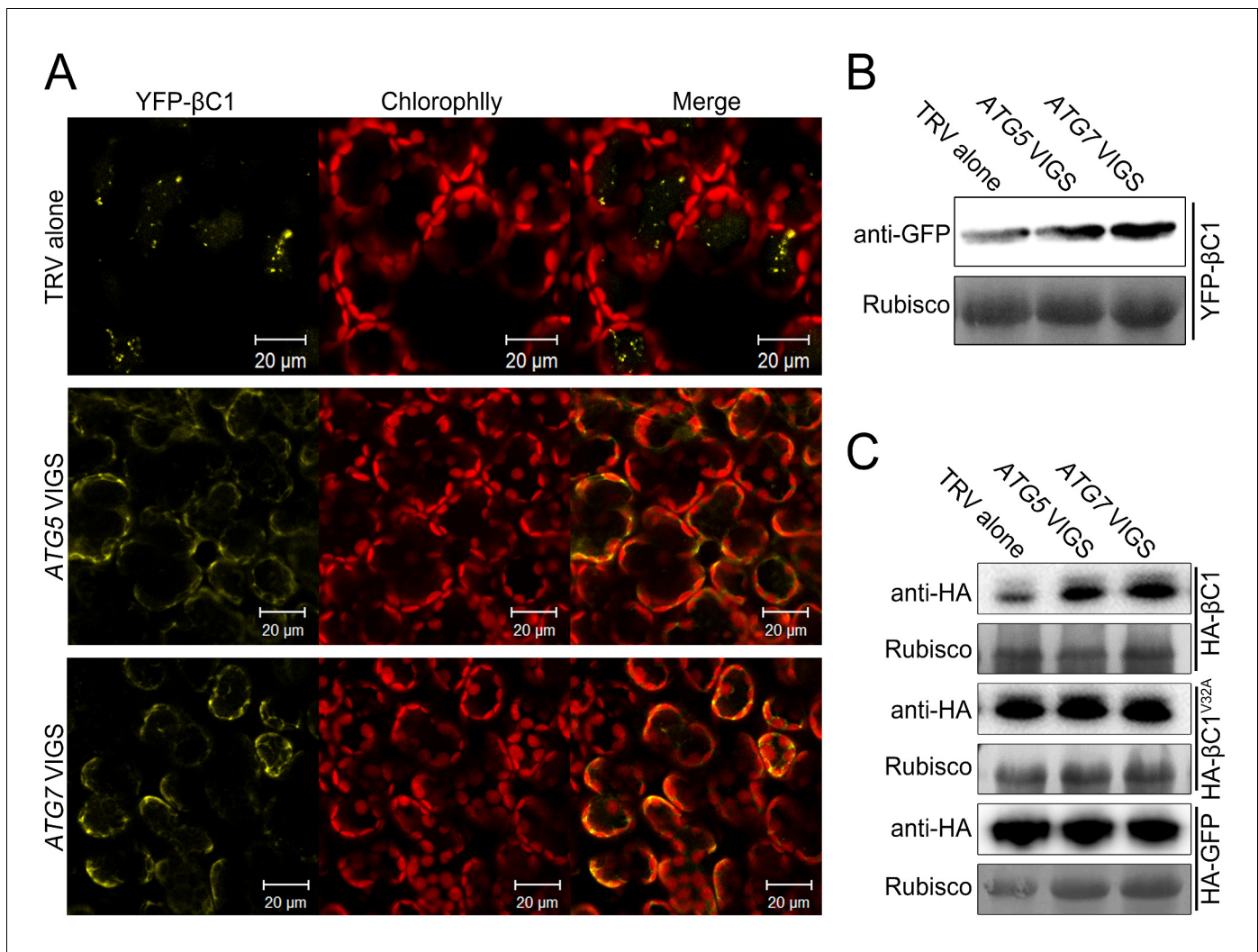


Figure 5. β C1 proteins is targeted for autophagic degradation. (A) Confocal microscopy images of YFP- β C1 in mesophyll cells of *N. benthamiana* leaves. YFP- β C1 was transiently expressed in non-silenced control (TRV alone), *ATG5* or *ATG7* silenced plants. The confocal microscope images of mesophyll cells were taken at 60 hpi. (B) Western blot analyses of YFP- β C1 construct from the same experiments as in (A). Level of the fusion protein, YFP- β C1, was detected with anti-GFP polyclonal antibody. (C) Silencing of either *ATG5* or *ATG7* enhanced the accumulation of HA- β C1, but not HA- β C1^{V32A}. Each expression constructs were agroinfiltrated into *N. benthamiana* leaf. At 60 hpi leaf lysates were separated by SDS-PAGE and fusion proteins were detected by anti-GFP or anti-HA antibodies.

DOI: [10.7554/eLife.23897.018](https://doi.org/10.7554/eLife.23897.018)

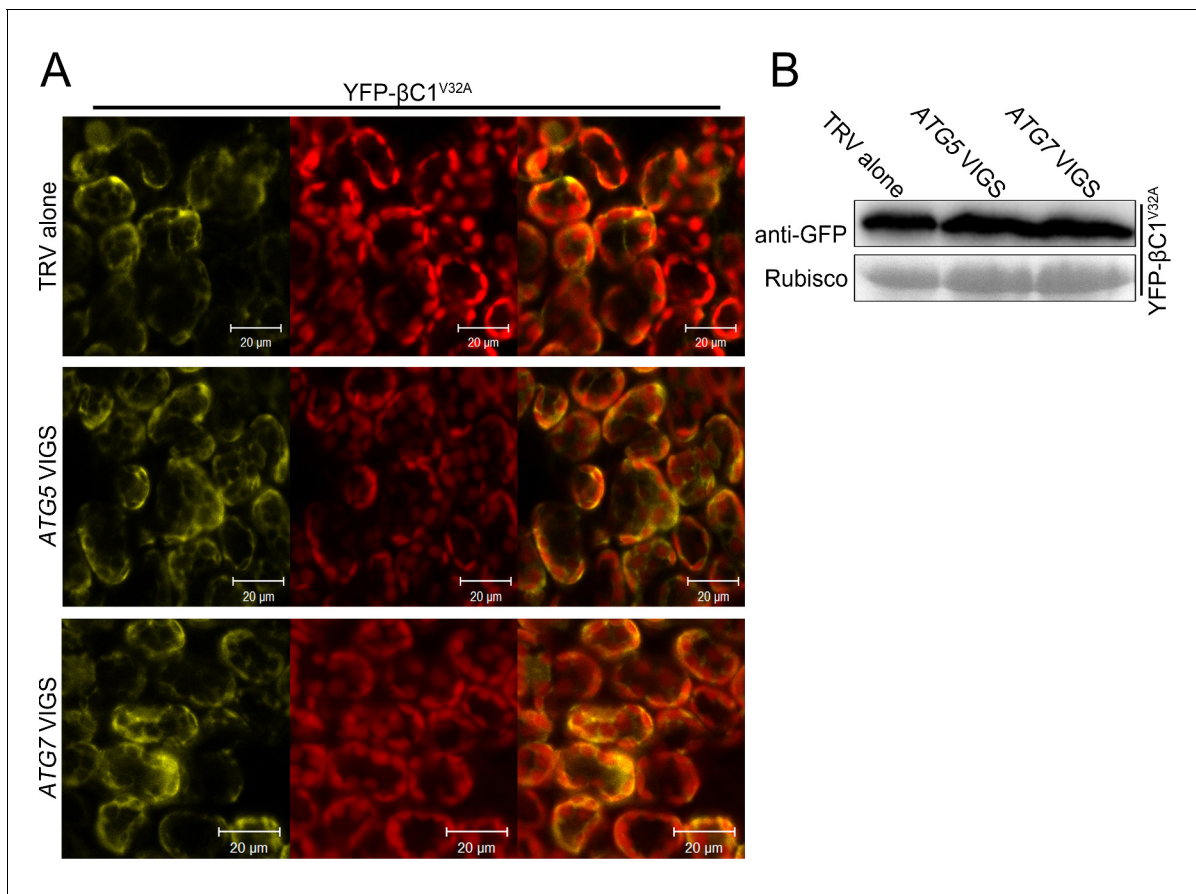


Figure 5—figure supplement 1. Silencing of either ATG5 or ATG7 has no effect on localization of YFP-βC1^{V32A}. (A) Confocal microscopy images of YFP-βC1^{V32A} in mesophyll cells of *N. benthamiana* leaves. YFP-βC1 was transiently expressed in non-silenced control (TRV alone), ATG5 or ATG7 silenced plants. The confocal microscope images of mesophyll cells were taken at 60 hpi. (B) Western blot analyses of YFP-βC1^{V32A} construct from the same experiments as in (A). Level of the fusion protein, YFP-βC1^{V32A}, was detected with anti-GFP polyclonal antibody.

DOI: [10.7554/eLife.23897.019](https://doi.org/10.7554/eLife.23897.019)

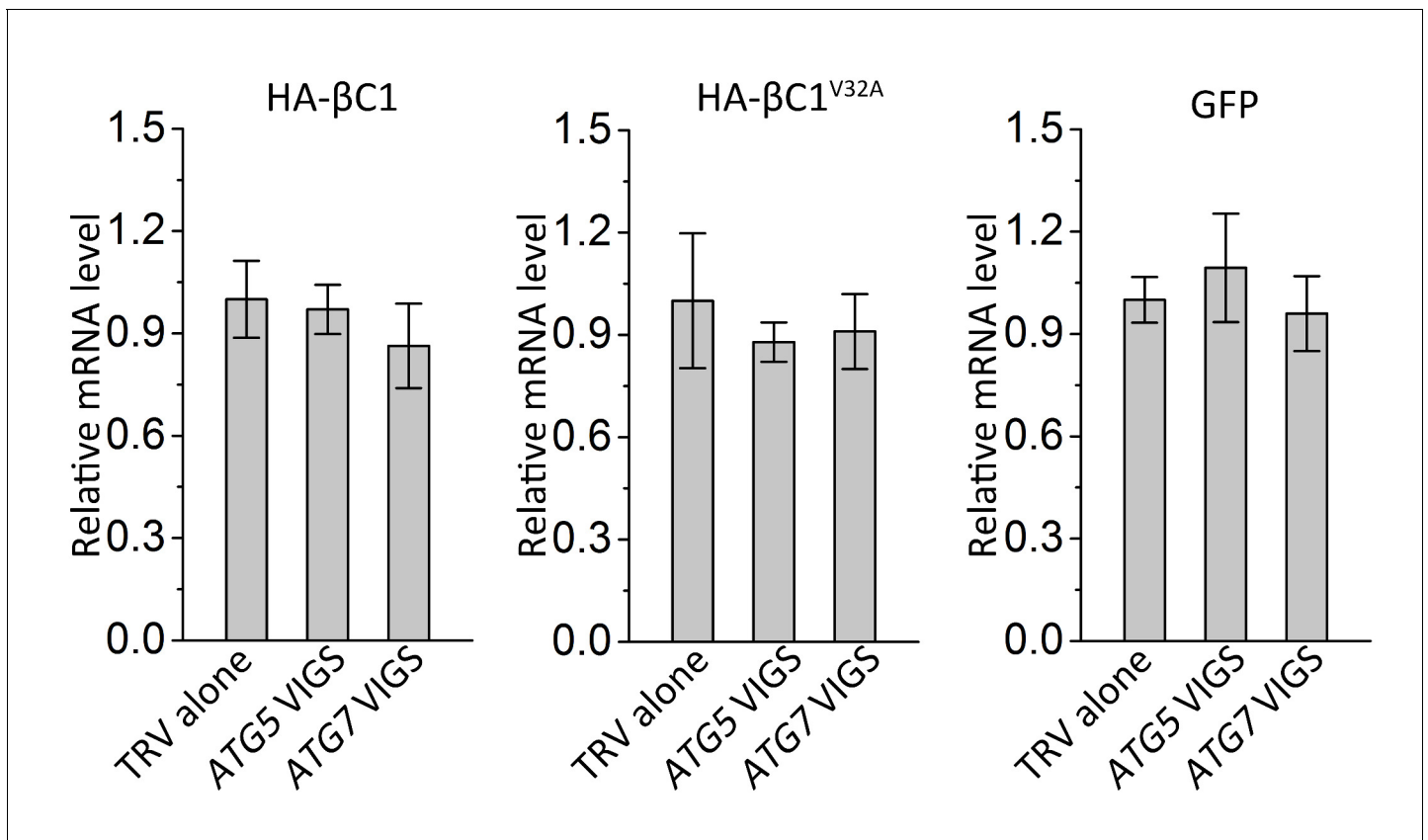


Figure 5—figure supplement 2. Silencing of either *ATG5* or *ATG7* has no effect on transcript levels of target genes. Real-time RT-PCR was performed to detect mRNA levels of target genes using gene-specific primers and total RNAs extracted from the infiltrated leaves of different plants. *eIF4α* was used as an internal control. Expression data relative to TRV alone groups are normalized to that of *eIF4α*. Values are means ± SE from three independent experiments. (*) $p < 0.05$.

DOI: [10.7554/eLife.23897.020](https://doi.org/10.7554/eLife.23897.020)

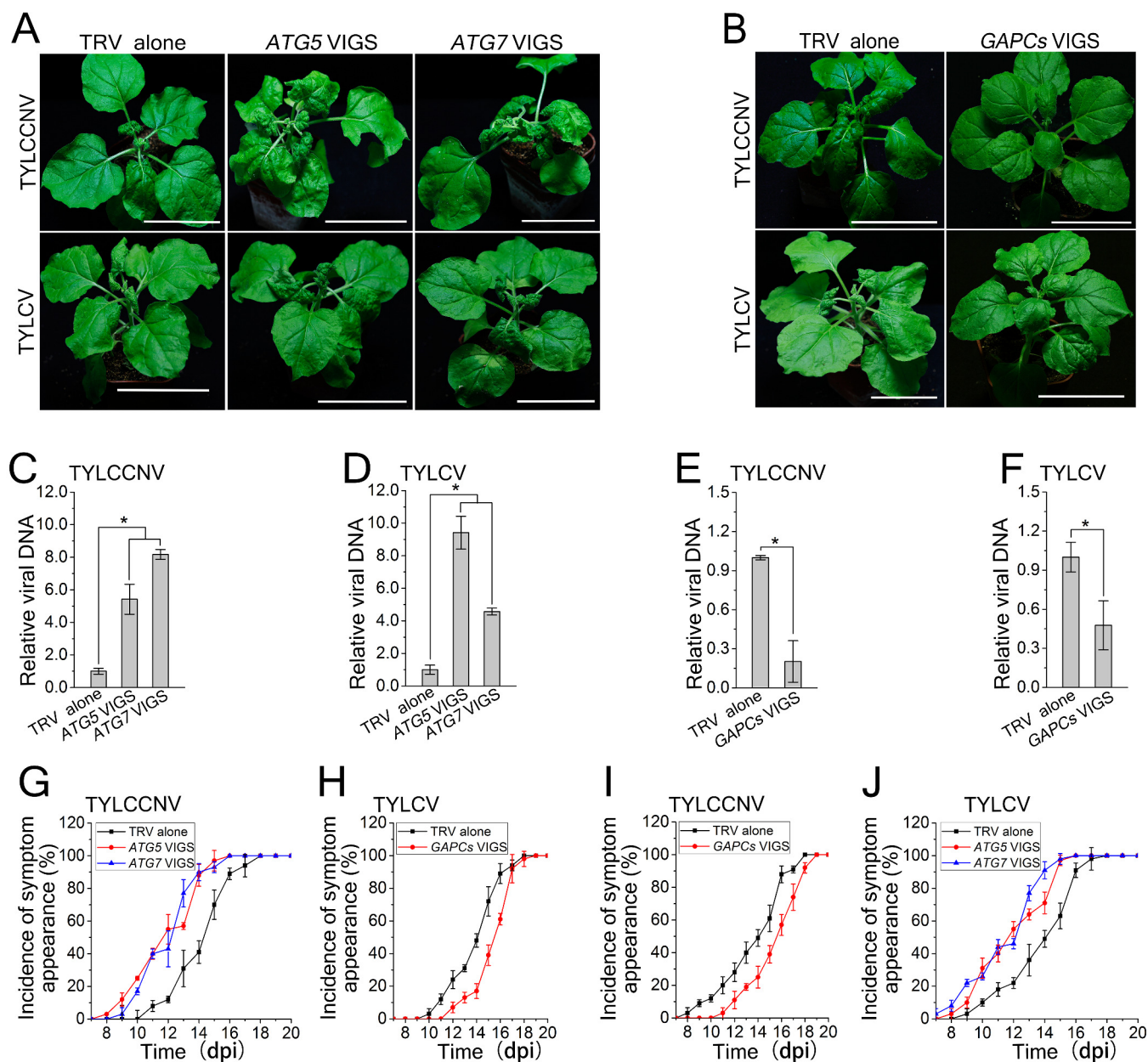


Figure 6. Autophagy regulates viral infection of TYLCV and TYLCCNV. (A) Viral symptoms in ATG5- and ATG7-silenced plants at 12 dpi. Bar represents 7 cm. (B) Viral symptoms in GAPCs-silenced (GAPCs VIGS) plants at 15 dpi. Bar represents 7 cm. (C) and (D) Relative viral DNA accumulation in ATG5- and ATG7-silenced plants. Real-time PCR analysis of V1 gene from TYLCCNV (C) or TYLCV (D) was used to determine viral DNA level in infected or control (TRV alone) plants. Values represent means \pm SE from three independent experiments. (*) $p < 0.05$. (E) and (F) Relative viral DNA accumulation in GAPCs-silenced plants. Real-time PCR analysis of V1 gene from TYLCCNV (E) or TYLCV (F) was used to determine viral DNA level in infected or control (TRV alone) plants. Values represent means \pm SE from three independent experiments. (*) $p < 0.05$. (G), (H), (I) and (J). The incidence of symptom appearance at different time points of post infection in VIGS plants. Symptom was indicated as the appearance of curled leaf caused by TYLCCNV in ATG5- and ATG7-silenced (G) and GAPCs-silenced (I) plants or TYLCV infection in ATG5- and ATG7-silenced (H) and GAPCs-silenced (J) plants. Values represent means \pm SE from three independent experiments.

DOI: [10.7554/eLife.23897.021](https://doi.org/10.7554/eLife.23897.021)

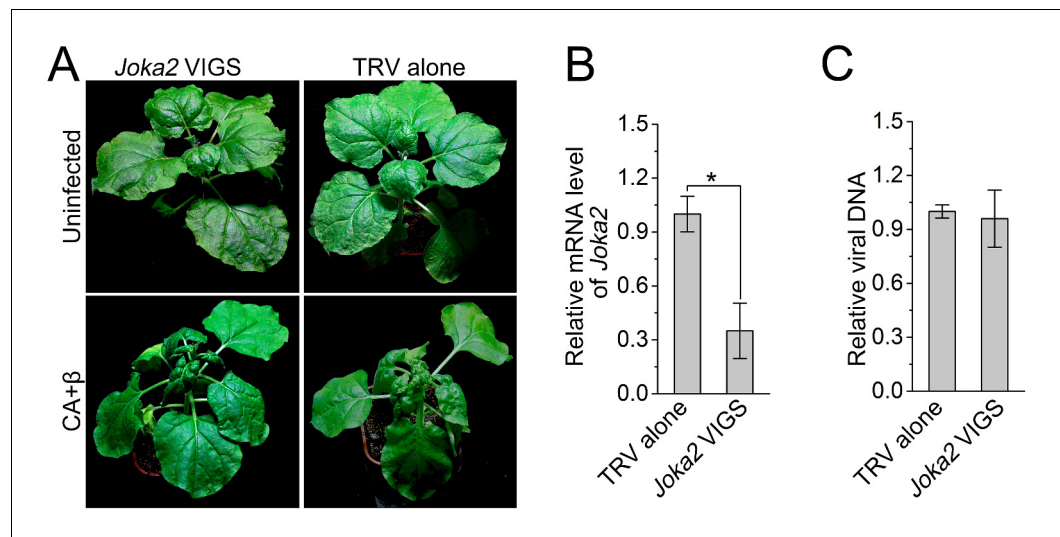


Figure 7. Silencing of *Joka2*, a plant selective autophagy cargo receptor, has no effect on CLCuMuV infection. (A) Viral symptoms in *Joka2*-silenced *N. benthamiana* at 12 dpi. (B) mRNA level of *Joka2* was reduced in *Joka2*-silenced plants. Real-time RT-PCR of *Joka2* was used to determine mRNA level. Values represent means \pm SE from three independent experiments. (*) $p < 0.05$. (C) Relative viral DNA accumulation in *Joka2*-silenced plants. Real-time PCR analysis of CLCuMuV V1 gene was used to determine viral DNA level. Values represent means \pm SE from three independent experiments. (*) $p < 0.05$.

DOI: [10.7554/eLife.23897.022](https://doi.org/10.7554/eLife.23897.022)